Spring 5-9-2020

Regulating Neuronal Growth with Structurally Defined Glycans

Gabriella D. Hartman
University of Mississippi

REGULATING NEURONAL GROWTH WITH STRUCTURALLY DEFINED GLYCANS

By

Gabriella Hartman

A thesis submitted to the faculty of the University of Mississippi in partial fulfillment of the requirements of the Sally McDonnell Barksdale Honors College.

Oxford

May 2020

Approved by:

_____

Advisor: Dr. Nicole Ashpole

_____

Reader: Dr. Joshua Sharp

_____

Reader: Dr. Kristopher Harrell

ACKNOWLEDGEMENTS

I would like to thank the Sally McDonnell Barksdale Honors College for enriching my academic experience and providing me with valuable resources, services, and staff these past four years. I would like to thank Dr. Ashpole for being an excellent mentor and instructing me throughout this project and teaching me how to employ leadership in the laboratory setting, as well as helping me grow as a woman in STEM. Thank you to Dr. Sharp and Dr. Pomin for also instructing me throughout this project and providing excellent feedback. Thank you to Jessica Marshall for always being helpful, and thank you to the rest of the Ashpole lab for encouraging me and helping me throughout this project. Thank you to my parents Lyudmila and Douglas Hartman, and my brother, Alex Hartman, for all your love and support. Without their encouragement, so few of my achievements would have been possible. Thank you to everyone else that has been so encouraging and loving throughout these past four years.

ABSTRACT
GABRIELLA HARTMAN: REGULATING NEURONAL GROWTH WITH STRUCTURALLY DEFINED GLYCANS
(Under the direction of Dr. Nicole Ashpole)

Chondroitin sulfate proteoglycans (CSPGs) and keratan sulfate proteoglycans (KSPGs) play an important role in neural development. Aggrecan, a CSPG, operates in the neural extracellular matrix where it negatively regulates neurite outgrowth to prevent aberrant process formation. Unfortunately, this aggrecan or CSPG-rich/KSPG-rich barrier can also prevent neuronal regeneration, which contributes to the inability to repair brain and spinal cord injuries. Removal of CSPGs and KSPGs has been shown to increase neurite outgrowth. We extend these findings by testing the ability of structurally-defined glycans to outcompete aggrecan and allow neurite outgrowth. Our overall goal is to determine if there is a particular glycan structure which can overcome inhibitory CSPGs and KSPGs without inhibiting neurite outgrowth themselves. We utilized primary cultures of rat neurons and applied polydisperse-related mixtures of CSPGs, KSPGs and newly-isolated, novel glycans in the absence and presence of aggrecan. Several of these glycans successfully removed the aggrecan-induced blockade while not inhibiting neurite outgrowth on their own. We are currently investigating the efficacy of these compounds in concentration-response curves and are testing additional glycans with different molecular weights and varying sulfation patterns to determine the structural requirements for the glycans as modulators of neurite outgrowth. By investigating the impacts of these glycans, we will increase the understanding of proteoglycan regulation of neural structure and function, and potentially identify compounds which could be used to treat spinal cord injuries.

Table of Contents Page

LIST OF IMAGES AND FIGURES

LIST OF ABBREVIATIONS

ANOVA	Analysis of Variance
CNS	Central Nervous System
CS	Chondroitin Sulfate
CSPG	Chondroitin Sulfate Proteoglycan
cDNA	Complementary DNA
DAPI	4’,6-diamidino-2-phenylindole
DNA	Deoxyribonucleic Acid
ECM	Extracellular Matrix
EL	*Echinometra lucunter*
ELHD	*Echinometra lucunter* Hydrolyzed
ELWD	Extra Long Working Distance
FBS	Fetal Bovine Serum
FITC	Fluorescein Isothiocyanate
GAG	Glycosaminoglycan
GalNAc	N-Acetylgalactosamine
GlcA	Glucuronic Acid
HA	Hyaluronic Acid
HBSS	Hank’s Balanced Salt Solution
IACUC	Institutional Animal Care and Use Committee
ISO	Isoflurane
KS	Keratan Sulfate
KSPG	Keratan Sulfate Proteoglycan

LAR	Leukocyte Common Antigen-Related
LVP1	*Lytechinus variegatus* Proteoglycan 1
LVP1HD	*Lytechinus variegatus* Proteoglycan 1 Hydrolyzed
LVP2	*Lytechinus variegatus* Proteoglycan 2
LVP2HD	*Lytechinus variegatus* Proteoglycan 2 Hydrolyzed
NMR	Nuclear Magnetic Resonance
NOE	Nuclear Overhauser Effect
PBS	Phosphate-Buffered Saline
PCR	Polymerase Chain Reaction
PFA	Paraformaldehyde
PLL	Poly-L-Lysine
PTPRF	Protein Tyrosine Phosphatase Receptor Type F
PTPRS	Protein Tyrosine Phosphate Receptor Type S
qPCR	Quantitative Polymerase Chain Reaction
RNA	Ribonucleic Acid
ROI	Region of Interest
RTN4R	Reticulon 4 Receptor
RTN4RL1	Reticulon 4 Receptor Like 1
RTN4RL2	Reticulon 4 Receptor Like 2
SCI	Spinal Cord Injury
SEM	Standard Error Measurement
TBI	Traumatic Brain Injury
TRITC	Tetramethylrhodamine

I. Background

When the body is injured, natural defenses begin to work to repair the damaged tissue. Inflammation, white blood cells, and a multitude of other factors combine to repair the damaged site. As with many tissues, a scar will form following injury (Beller, 2014). Traumatic brain injury (TBI) or spinal cord injury (SCI) lead to the formation of specific type of scar tissue called glial scars, which are comprised of complex molecular interactions and are poorly understood. Glial cells, the principal cells responsible of the formation of glial scars, are a group of essential cells within the nervous system that respond to injury and provide structural and metabolic support. Glial cells include astrocytes, oligodendrocytes, and microglia. Following a SCI, specialized astrocytes will coordinate the healing process and form the glial scar along with connective tissue. Previous studies have shown the importance of the response of glial cells to injury and the implications for permanent damage as a result. The glial scar acts as a protective, yet inhibitory barrier, preventing regeneration of the spinal cord, ultimately leading to permanent effects like paralysis (Daniell, 2012). Though it was commonly thought before that the glial scar was a mechanical barrier to neuronal regeneration, it is now understood that the upregulation of certain molecules in the glial scar may allow for neuronal regeneration (Daniell, 2012). Because both TBI and SCI result in axonal injury, it is thought that identification of molecules or mechanisms that permit axonal repair through the scar may have the potential to improve outcomes following these injuries (Harris, 2009).

A major factor contributing to the inhibition of neurite outgrowth and regeneration is the upregulation of inhibitory chondroitin sulfate (CS) and keratan-sulfate (KS)

proteoglycans (CS/KSPGs) following a traumatic injury. Proteoglycans are glycoproteins that have glycosaminoglycans (GAGs) attached and are a key component in the extracellular matrix (ECM). They comprise nearly 20% of the ECM and are known to have a role in the progression of disease, cell proliferation, and nervous system development (Djerbal, 2017). GAGs are highly anionic linear polymers composed of disaccharide units of either uronic acid or galactose and a hexosamine (Pomin, 2012). CSPGs contain a carbohydrate chain with alternating N-acetylgalactosamine (GalNAc) and glucuronic acid (GlcA) units with varying sulfation patterns, whereas KSPGs are poly-N-acetyllactosamine chains (Varki, 2017). Together, CS/KSPGs also have glycan chains varying in size, number, and sulfation patterns which allow for vast diversity in the effects of CS/KSPGs on neurite regeneration and rehabilitation. Proteoglycans can affect neurite outgrowth through interactions of the core protein and the GAG chains. These interactions regulate various physiological processes such as inflammation, metastasis, development, regeneration, coagulation, cell adhesion, growth, and neuronal regeneration (Pomin, 2012). Though both core protein and GAG chain interactions have been shown to impact neuronal growth, the mechanism by which these affect neuronal regeneration is not well understood (Beller, 2014). However, the regulation of neurite outgrowth is thought to be receptor mediated mechanisms – likely through RTN4R, RTN4RL1, PTPRF, etc. It is unclear whether the CS/KSPGs interact with the receptor either directly or indirectly (Daniell, 2012). Regardless, upregulation of proteoglycans following injury in the CNS is indicative of decreased neurite outgrowth and a nonpermissive growth environment, providing an opportunity for the introduction of a possible therapeutic intervention (Daniell, 2012).

Although the mechanism of CS/KSPGs and its inhibitory effects on neuronal plasticity is largely unexplored and not completely understood, there is evidence that disruption of the CS/KSPG interactions will increase neurite outgrowth and regeneration. Aggrecan from bovine cartilage (a CS/KSPG) sufficiently inhibits axon outgrowth in an *in vitro* culture model, and this inhibitory effect is lost following digestion of the CS GAG chain or by alterations of the core protein (Ohtake, 2015). When aggrecan binds to hyaluronic (HA), an important component of articular cartilage, large negatively charged aggregates are formed (**Figure 1**) (Holmes, 1988). The ability of aggrecan to form aggregates of hyaluronan (HA) and other properties are attributed to its high content of CS (Collin, 2017). But, since aggrecan contains little KS, it is likely that the ability of CS/KSPGs to inhibit neurite regeneration is due to the proper spatial presentation of both KS and CS.

There is considerable diversity in glycan structure found in nature and it is known that sulfated glycans from marine life have the potential biotherapeutic functions in the organisms that produce them and exogenously in other organisms (Pomin, 2014). Sulfated fucans from sea urchin egg jelly express variability in structure and sulfation patterns among species. This species-specific differentiation regulates fertilization by inducing an acrosomal reaction with only compatible sperm. Thus, structural changes in glycans of the sea urchin egg jelly may lead to speciation and evolutionary changes, as changes in the glycan structure ultimately leads to incompatibility between sperm and egg.

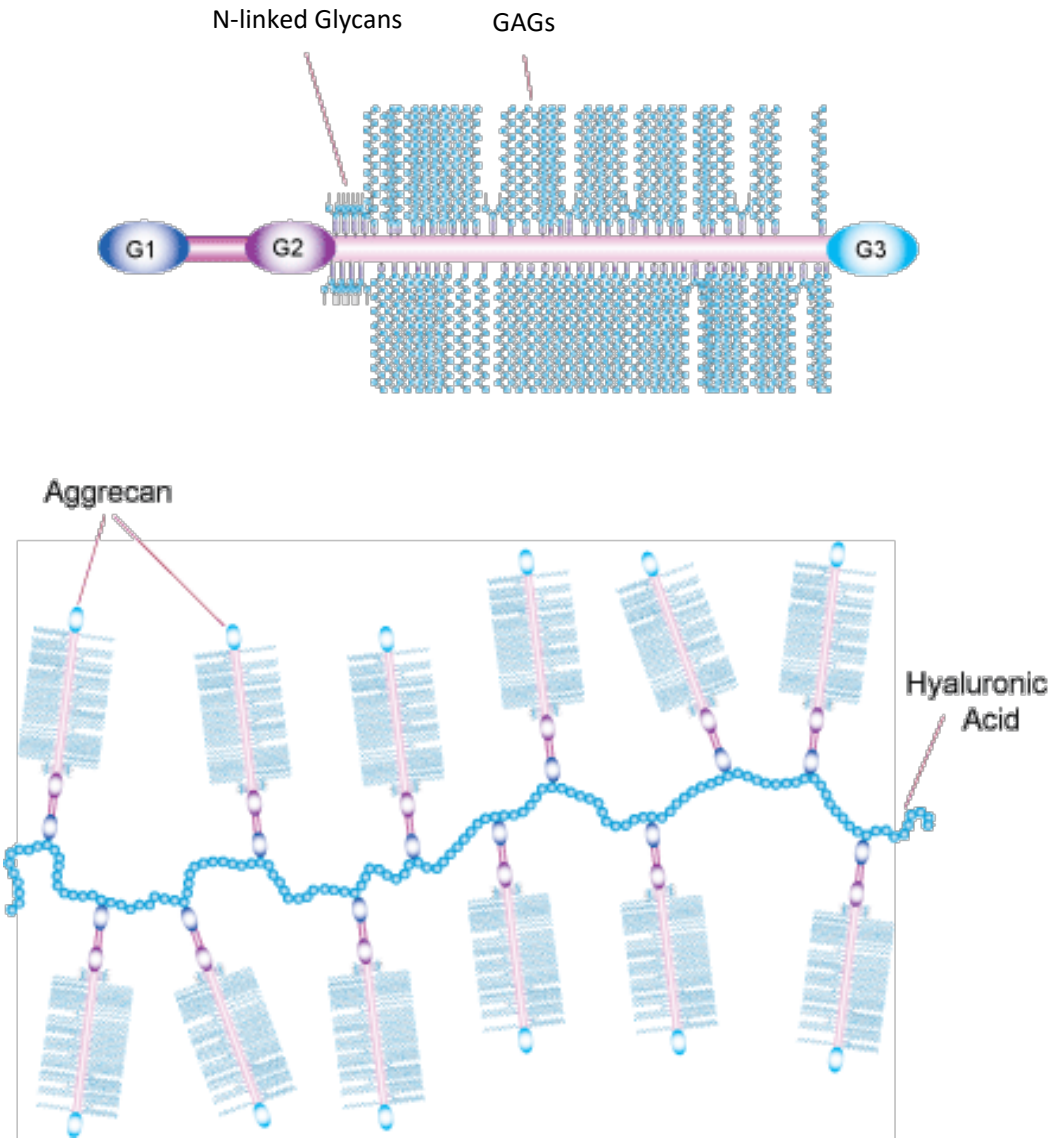

Figure 1: Structure of Aggrecan. Source(s): Millipore Sigma, [Structural Proteins – Aggrecan]. Retrieved from https://www.sigmaaldrich.com/life-science/metabolomics/enzyme-explorer/learning-center/structural proteins/aggrecan.html.

We sought to examine whether novel glycans isolated from these sources can outcompete CS/KSPGs such as aggrecan and ultimately regulate neuronal growth. To do this, unique glycans from *Lytechinus variegatus* (*L. variegatus)* and *Echinometra lucunter* (*E. lucunter*) were investigated in their effect on neuronal growth and competition with CS/KSPGs. Two glycans were extracted and tested from the egg jelly of *L. variegatus*, LVP1 and LVP2, and one glycan was extracted from *E. lucunter*, along with their low molecular weight derivatives. LVP1 is a high molecular polymer of [L-Fuc*p*4(SO_3^-)-α(1-3)-L-Fucp2,4(SO_3^-)-α(1-3)-L-Fuc*p*2(SO_3^-)-α(1-3)-L-Fucp2(SO_3^-)]n. The presence of electrostatic repulsion of the sulfates in the linking disaccharide [-3)-α-L-Fucp-2(OSO3)-(1–3)-α-L-Fucp-4(OSO3)-(1-] between the tetrasaccharides accounts for the increased motion in the glycan structure (Queiroz, 2015). LVP2 is a high molecular weight polymer composed of [L-Fuc*p*4(SO_3^-)]n, while the glycan from *E. lucunter* is composed of [L-Gal2(SO_3^-)]n. All native forms are close to 100 kDa. Low molecular weight derivatives were acquired by hydrolysis of native glycans. Hydrolyzed *E. lucunter* glycans (ELHD) are composed of 60% [→3)-α-galactose(2SO_3^-)-(1→]n and 40% [→3)- α-galactose-(1→]n, and hydrolyzed LVP2 (LVP2HD) are composed of 80% [→3)- α-fucose(4SO_3^-)-(1→]n and 20% [→3)- α-fucose-(1→]n and 20% [→3)- α-fucose-(1→]n. Therefore, the low molecular weight derivatives contain essentially the same structure as the native form, but with less sulfation.

CS, the core protein of CSPGs, is the most abundant GAG endogenously produced in the central nervous system and consists of repeating disaccharide units of D-glucuronic acid (GlcA) and N-acetylgalactosamine (GalNAc). Various positions of CS may be sulfated, giving rise to different residues of CS. For example, sulfation of C-4 of

GalNAc gives rise to CS-A, C-6 of GalNAc gives rise to CS-C, C-2 of GlcA and C-6 of GalNAc gives rise to CS-D, and C-4 and C-6 of GalNAc gives rise to CS-E (Djerbal, 2017). The sulfation patterns are vital to consider when investigating the interactions between glycans of CS/KSPGs and neurons (Queiroz, 2015). Thus, prior to testing the functional effects of these glycans in our neuron cultures, our collaborators conducted NMR analysis to verify sulfation patterns, thereby allowing us to determine structure-function relationships. It was determined that the CS preparation was approximately 50% non-sulfation and approximately 50% 6-sulfation, indicating our novel glycans primarily featured CS-C.

Other factors that influence glycan interactions with target cells are glycan dynamics and conformation; however, little information on this is known on the exact size and shape required for regulating neurons. There is a vast amount of diversity in glycan size, shape, and sulfation pattern observed in nature. We set out to assess the conformations and sulfation patterns may be serve as important biological regulators within the ECM. We hypothesize that specific sulfated glycans isolated from sea urchins will outcompete aggrecan and allow neurite outgrowth and that disruption of CSPG and/or KSPG signaling will promote axonal regeneration. We tested a variety of mammalian and marine sulfated glycans with unique structures and examined their impact on neurite outgrowth. As controls, chondroitin sulfate (CS), chondroitinase, enoxaparin, and heparin were examined as studies have shown that enzymes such as keratanase and chondroitinase, as well as low molecular weight glycans prove to effectively inhibit CS/KSPGs are restore growth following a SCI (Barriett et al., 2006, Kim et al., 2006). Examining the both protein-GAG interactions and sulfation patterns in

our neuronal growth assays may provide insight on the molecular mechanisms underlying the regulation of neurite growth and regeneration (Pomin, 2012). This comprehensive study of novel glycans, proteoglycan regulation, and growth of neurite processes has the potential to provide insight into the mechanism by which CS/KSPGs operate and be a resource to support further studies aimed at treatment and rehabilitation following a TBI or SCI.

II. Methods

Animals

All animal procedures were approved by the Institutional Animal Care and Use Committee (IACUC) at the University of Mississippi and performed in accordance with their approved guidelines. Timed-pregnant Sprague Dawley rats were ordered from Envigo and arrived into the UM animal care facility at 17 days postcoitum and were temporarily housed with access to food (Teklad 7001) and water ad libitum until the time of euthanasia (described below). Cerebral tissue of both male and female pups were utilized in the study.

Coating Plates

96-well or 24-well plates were precoated with 0.01% Poly-L-Lysine (PLL) prior to starting cell culture to give the neurons a surface to attach to in the wells. After 24 hours in an incubator, the PLL was removed and washed 3 times with HPLC-grade water. The plates were then treated with aggrecan and/or the novel glycans at various concentrations, as indicated on the respective figures. The plates with glycans were then incubated at 37°C for 4 hours to allow adherence. The treatment was removed, and the plates were washed with HPLC water three times, vacuuming off the HPLC water after each wash.

Culturing Neurons

Pregnant Sprague Dawley rats were euthanized 17 days postcoitum with isoflurane anesthesia followed by cervical dislocation. The ventral side of the rat was then cleaned with ethanol. The embryos were removed and placed into a 10 cm dish on ice with Hank's Balanced Salt Solution (HBSS). To extract the neurons, a midsagittal

incision was made down the brain and transversely across the occipital bone. After extracting the brain from the embryos, the hemispheres were separated, the meninges were removed, and then placed into 15mL conical with 1X HBSS. HBSS was then removed and added Papain/HBSS solution for 20-25 minutes in the incubator to enzymatically digest the tissue. After incubation, Papain/HBSS solution was removed.

The neurons were washed with pre-warmed Neurobasal media, 45 mL FBS, L-Glutamine, and 5 mL pen strep three times before being titurated with media using a glass pipette. The supernatant was run through the filter and remaining brains were titurated two more times. The neurons were plated with a cell density of 250,000 cells/cm^2 in each pre-treated well, then incubated at 37°C in the presence of 5.0% CO_2 for 24 hours. After 24 hours, the media was replaced with new neurobasal media with B27 supplement, L-Glutamate, and 5 mL pen strep and continued to incubate for another 24 hours (Ashpole, 2011). After culturing neurons on the pre-treated plates, they were placed in an incubator at 37°C and 5% CO_2 for 48 hours.

Immunostaining Cells

Forty-eight hours after incubation, cells were fixed with 4% paraformaldehyde (PFA) in phosphate buffer for 20 minutes and permeabilized with 0.1% Triton X-100 in PBS for 20 minutes. Then, cells were blocked with 0.1% Triton X-100 in PBS with 5% bovine serum albumin (BSA) for 1 hour, immunostained with anti-β-Tubulin antibody (Cell Signaling Technology, Rabbit mAb, 2128S, 1:100) in PBS overnight at 4°C. Following removal of the primary antibody, the wells were washed 3 times with PBS for 5 minutes and treated for 1 hour in the dark with a 488 nm fluorescent goat anti-rabbit (ThermoFisher, 1:1000). Plates were then rinsed three times with PBS for 5 minutes and

treated for thirty minutes in the dark with DAPI (ThermoFisher, EN62248, 1:1000). Plates were again rinsed three times with PBS for 5 minutes and stored in PBS.

MTS Assay

CellTiter 96® AQ_{ueous} One Solution Reagant was used to perform the MTS to determine the viability of the cells left on the plate following treatment. Active cells will metabolize the reagent and change it to formazan, thus changing the color form a pale yellow to a dark purple, allowing detecting of viable cells with visible light. The reagent includes tetrazolum, as well as electron coupling reagents to reduce the reagent to eventually form the indicative formazan (Riss, et al., 2013). After the CellTiter 96® AQ_{ueous} One Solution Reagant was added to the wells, the plates were placed in the incubator for 1-2 hours once an obvious color change from pale yellow to dark purple was observed. The plate was then placed in a plate reader and read at an absorbance of 490 nm.

Gene Expression

A subset of cells was grown for seven days to examine long-term changes in structure and gene expression. These cells were cultured on 6cm round dishes until RNA was isolated using the RNeasy kit. For this, 350 µl of Buffer RLT was added per dish. Plates were scraped and the cells and Buffer RLT were pipetted in spin columns. Samples were centrifuged for 15 seconds at 8000 x g and flow through was discarded. 700 µl of Buffer RW1 was added and centrifuged for 15 seconds at 8000 x g, then flow through was discarded. Then, 500 µl of Buffer RPE was added to the spin columns and centrifuged at 8000 x g for 15 seconds. This step was repeated, but the samples were centrifuged for 2 minutes instead. Flow through was discarded between each step.

Samples were then centrifuged again at full speed for 1 minute to dry the membranes. Following this, approximately 50 µl of RNase-free water was added to the spin column, and samples were spun in the centrifuge at 8000 x g for 1 minute to remove the RNA from the column. Nanodrop RNA was used to identify concentration and purity of samples. Then, Applied Biosystems High Capacity RNA-to-cDNA Kit was used to convert RNA samples to cDNA, and TaqMan Universal PCR Master Mix and TaqMan gene specific primers (PTPRS, PTPRF, RTN4R, RTN4RL1, RTN4RL2) were used to run a real-time PCR and was ran for 40 cycles.

Imaging

Following staining, multi-well plates were imaged on a High Content Analysis Nikon Ti2-E Microscope with CSI S Plan Fluor ELWD 20x Ph1 ADM objective with DAPI (395 nm) and FITC (470 nm) fluorescent filters, or with Plan Apo λ 60x Oil objective with DAPI (395 nm), FITC (470 nm), and TRITC (532 nm) fluorescent filters with 200 ms exposure. Image locations were selected at random.

Image Analysis

All data was saved and exported using Excel (Microsoft Office, 2016). Sholl Analysis was used to trace neurites and count number of neurite crossings (**Figure 2**). Concentric ring distance was then used to generate a curve and calculate the area under the curve as a representation of total neurite outgrowth (ImageJ).

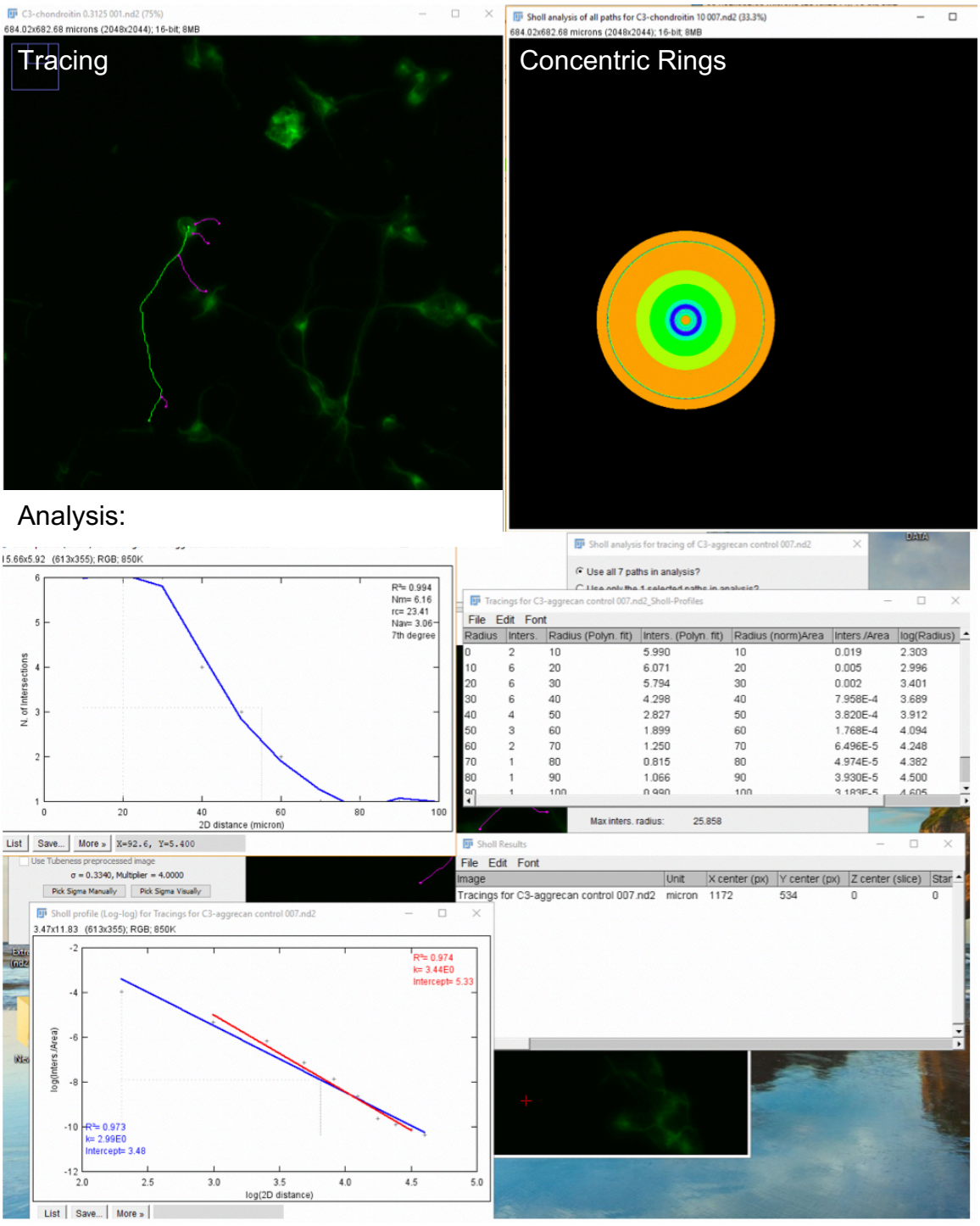

Figure 2: Representative image of steps of Sholl analysis to assess total neurite outgrowth as stated above. ImageJ was used to trace all processes of neuron, with primary process in green and additional processes in purple. Concentric ring distance was then used to assess total crosses over a certain distance, followed by various calculations and area under the curve analysis.

Nikon Elements Analysis software object count was used to measure the total percent area of green fluorescence (neurites) and normalized it to blue fluorescence (nuclei) to confirm the total neurite outgrowth (NIS Elements AR Analysis, Version 5.02). SigmaPlot was used to create all graphs and run statistical analysis (Systat Software, San Jose, CA). In the graphs, error bars were used to represent plus/minus standard error measurement (± SEM) in cases where data was averaged.

Statistical Analysis

The data was evaluated by one-way analysis of variance (ANOVA) using multiple groups. A Dunnett's *post hoc* test using SigmaPlot was also used to verify statistical significance of groups in comparison with the control (Systat Software, San Jose, CA). All data was normalized to the control in SigmaPlot. Curve fitting was done using a 4-parameter logistic sigmoidal curve. Results were considered statistically significant if $p < 0.05$.

III. Results

Neuron cultures were established from rat cortices and grew cell *in vitro* for two days following treatment of plates for 48 hours with varying concentrations of aggrecan. After developing neurons in culture, the neurons were fixed with paraformaldehyde and stained using immunocytochemistry techniques and then imaged. Total neurite growth was assessed using various methods of analysis to confirm aggrecan inhibits neuronal growth at increasing concentrations, as previously demonstrated in other publications (Johnson, 2002). Sholl analysis was used to determine what concentration of aggrecan statistically significantly inhibits neuronal growth (**Figure 3C**). Because each row of the 24-well plate was treated with a different concentration of aggrecan, the graph represents the average area of neuron processes per nuclei. All data was normalized to the control. As the concentration of aggrecan increased, there was a significant decrease in neurite outgrowth at 5.0, 7.5 and 10.0 micrograms/milliliter of aggrecan. Further analysis of total neurite growth following with increasing concentrations of aggrecan was assessed using area of neurite coverage and longest neurite quantification, and the results indicated that 7.5 and 10.0 micrograms/milliliter of aggrecan significantly inhibited neurite outgrowth (**Figure 3D-E)**. From this, it was determined that 10 micrograms/milliliter of aggrecan would be used as a standard concentration of aggrecan in this experiment. All other treatments with aggrecan therefore have a concentration of 10 micrograms/milliliter unless stated otherwise.

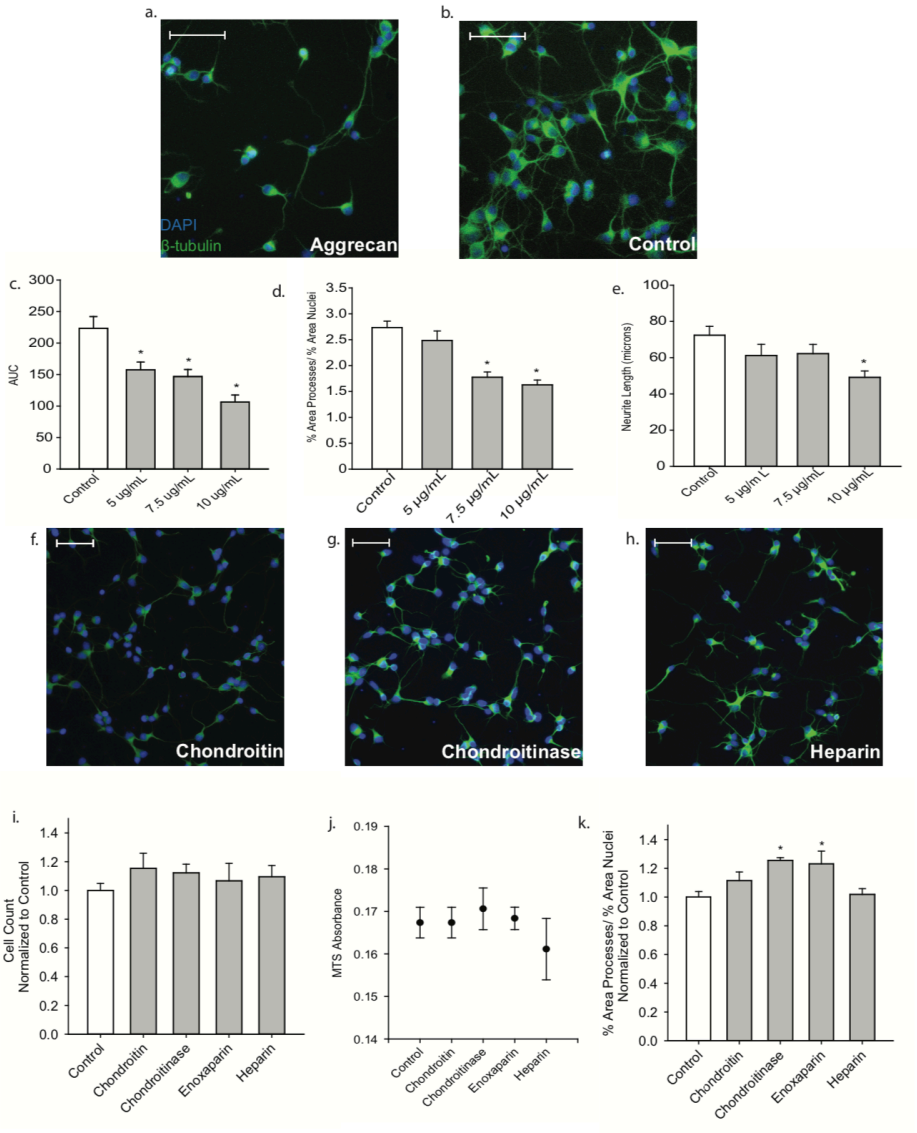

Figure 3: Increasing concentration of aggrecan exhibited neurite outgrowth inhibition, while known glycans do not inhibit neurite outgrowth. (a) cortical neuron cells were cultured at 250,000 cells/cm^2 and treated with 10 μg/mL aggrecan. Neurons were fixed and stained with β-tubulin (green) and DAPI (blue). Scale bar represents 50 μm. (b) cortical neurons treated with water for control, scale bar represents 50 μm. (c) Sholl analysis of neurons treated with water, 5 μg/mL, 7.5 μg/mL, and 10 μg/mL of aggrecan. *, $p < 0.05$, n=12 (d) area analysis of cortical neurons treated with water, 5 μg/mL, 7.5 μg/mL, and 10 μg/mL of aggrecan. *, $p < 0.05$, n=12 (e) neurite length of cortical neurons treated with water, 5 μg/mL, 7.5 μg/mL, and 10 μg/mL of aggrecan. *, $p < 0.05$, n=12 Representative images of cortical neurons treated with chondroitin (f), chondroitinase (g), and heparin (h). Scale bars represent 50 μm. (i) cell count normalized to control of known glycans chondroitin, chondroitinase, enoxaparin, and heparin. n=8-16 (j) MTS absorbance assay of known glycans to test for toxicity, n=8 (k) area analysis of known glycans normalized to control, n=8-16

In comparison to aggrecan's inhibitory effect on neurite outgrowth, cortical neurons treated with 10 micrograms/milliliter of known glycans alone revealed that these glycans do not inhibit neurite outgrowth, nor did these glycans decrease number of nuclei (**Figure 3I, K**). An MTS absorbance assay was also conducted on cells treated with these glycans to further to assess viability, and results support that these glycans had no toxicity effects on the neurons (**Figure 3J**).

Novel sulfated glycans from marine life were then applied to the culture plates (10 micrograms/milliliter) prior to the addition of cortical neurons. These novel glycans and derivatives were provided by Dr. Vitor Pomin. Forty-eight hours after plating neurons were analyzed by cell count, area analysis, and for neuronal viability to confirm that novel glycans alone did not contribute to toxicity for neurons (**Figure 4G, H, I**). Results showed that novel glycans did not significantly alter number of nuclei, nor did they contribute to toxicity. LVP2HD did, however, show an increase in metabolic activity compared to other glycans (**Figure 4H**). Additionally, novel glycans did not exhibit a decrease in total processes following area analysis, and treatment of ELHD, LVP1HD, and LVP2HD alone, without the presence of inhibitory molecules showed a significant increase in total processes per cell (**Figure 4I**). Structures of novel glycans are exhibited, with R in *E. lucunter* representing at sulfated group in EL, and is 60% sulfated in ELHD. R in LVP2 represents a sulfate group, while being 80% sulfated in LVP2HD (**Figure 4A, B, C**). Sulfation patterns for LVP1HD exhibit undefined selective sulfation.

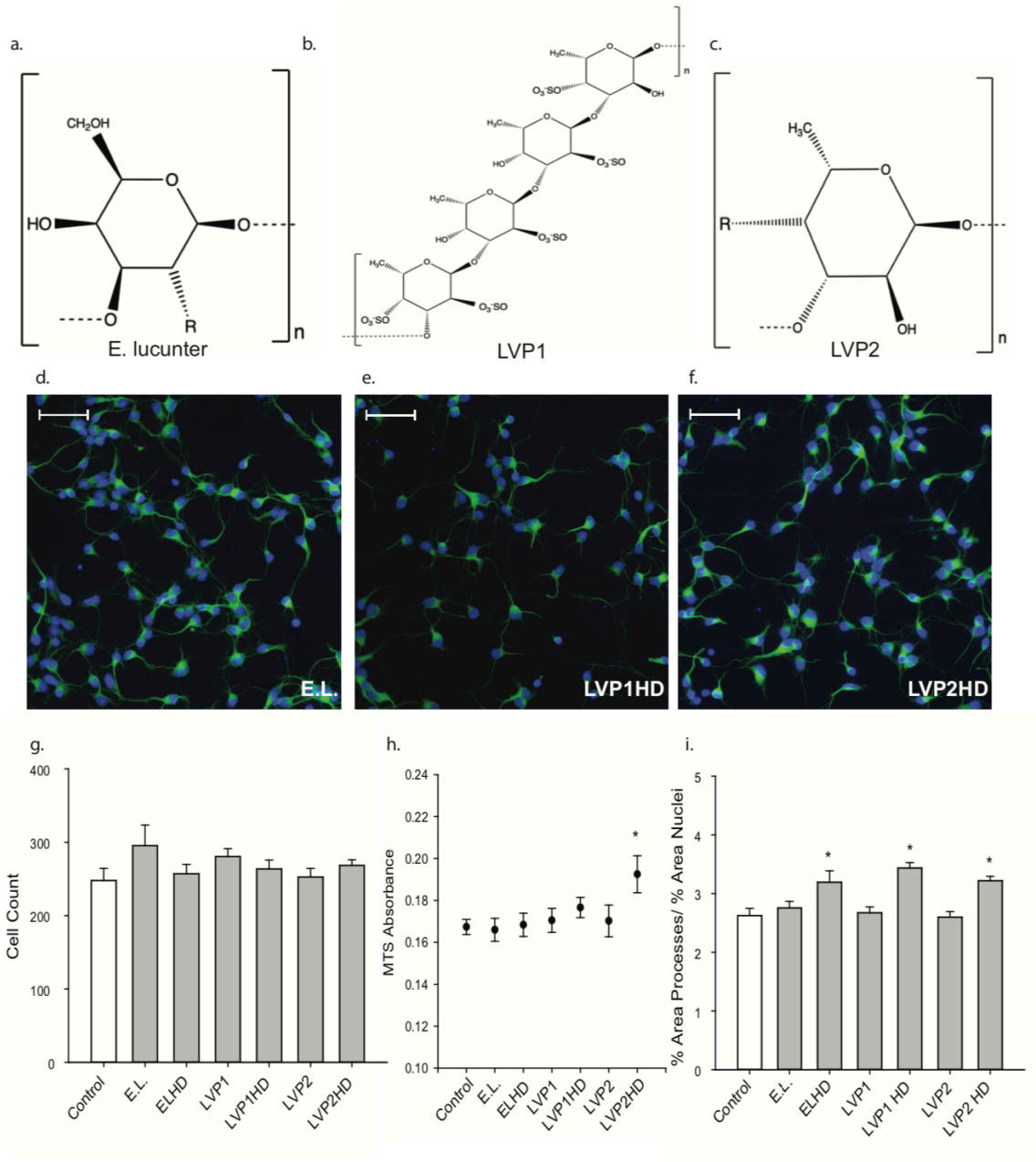

Figure 4: Novel sulfated glycans do not inhibit neurite outgrowth. (a) structure of α-galactose 2 sulfate glycan from E. lucunter, R=60% OSO_3^- and 40% H for ELHD. (b) structure of novel glycan from LVP1 (c) structure of 3-linked 4-sulfated α-fucan glycan from LVP2, R=80% OSO_3^- and 20% H for LVP2HD. Representative images of cortical neurons treated with 10 μg/mL of E.L (d), LVP1HD (e), and LVP2HD (f). Scale bars represent 50 μm. (g) nuclei count of cortical neurons treated with 10 μg/mL of novel glycans, n=8 (h) MTS absorbance assay of cortical neurons treated with 10 μg/mL of novel glycans, *, $p<0.05$, n=8 (i) area analysis of cortical neurons treated with 10 μg/mL of novel glycans, *, $p<0.05$, n=8

Next, the protective ability of various novel glycans were tested against 10 micrograms/milliliter of aggrecan at the same concentration used in Figure 4 to demonstrate the ability of novel sugars to outcompete aggrecan. Images were analyzed using sholl analysis and nuclei count. After completing sholl analysis, the number of neurite crossings from the soma were plotted, then the area under each curve was integrated and calculated to generate a bar graph. For these sets of data, an ANOVA statistical analysis was run with a Dunnett's *post hoc* test to determine which glycans significantly outcompeted aggrecan's inhibitory influence on the neuron culture. Again, all data was normalized to control and error bars representing ± SEM. Sholl analysis revealed that EL, ELHD, LVP1HD, LVP2, and LVP2HD, statistically outcompeted aggrecan and allowed for neurite growth (**Figure 5E**). Additionally, nuclei count of neurons treated with both novel glycans and aggrecan was conducted (**Figure 5F**). From this, it was determined that LVP1HD and LVP2HD allowed for an increase in nuclei count as well.

Following this, it was hypothesized that these novel glycans allow for neurite outgrowth in a concentration dependent manner (Snow, 1992). Before beginning concentration response curves with the novel glycans, potency of chondroitin on neuronal growth was tested, as it has been previously published in literature that chondroitin allows for growth in a concentration-dependent manner. Various concentrations of chondroitin were applied to neurons and viability was assessed using area analysis (**Figure 6E**).

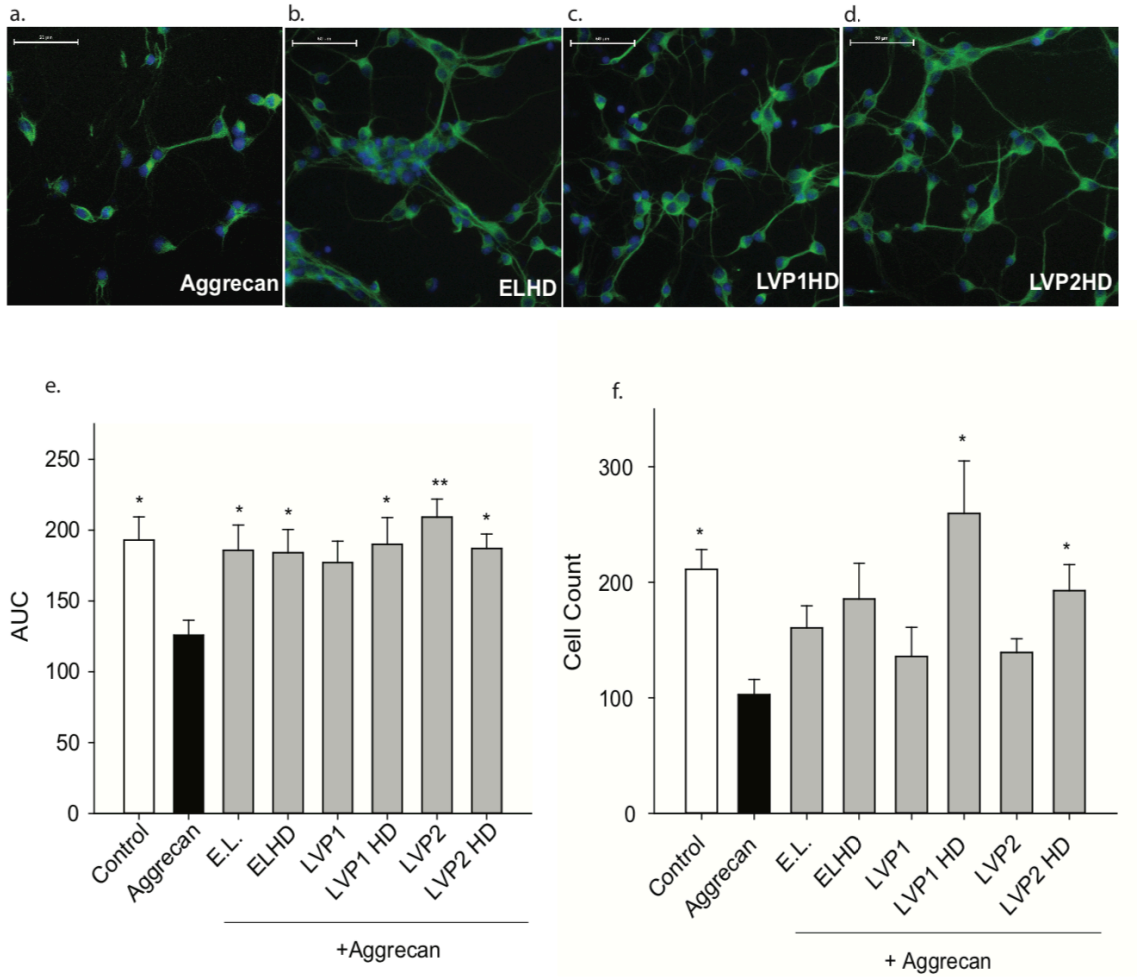

Figure 5: Novel glycans outcompete aggrecan. Representative images of cortical neurons treated with 10 μg/mL aggrecan (a), 10 μg/mL aggrecan + 10 μg/mL ELHD (b), 10 μg/mL aggrecan + 10 μg/mL LVP1HD (c), and 10 μg/mL aggrecan + 10 μg/mL LVP2HD (d). Scale bars represent 50 μm. (e) area under the curve from sholl analysis of cortical neurons treated with 10 μg/mL aggrecan + 10 μg/mL novel glycans; *, $p< 0.05$, **, $p>0.001$, n=12 (f) nuclei count of cortical neurons treated with 10 μg/mL aggrecan + 10 μg/mL novel glycans; *, $p<0.05$, n=6

Concentrations of 0.15625 to 20.0 micrograms/milliliter of chondroitin was applied and data was assessed again using a one-way ANOVA with Dunnett's *post hoc* test vs control. All data was normalized to control. From this assay, it was determined that concentrations exceeding 2.5 (5.0, 10.0 and 20.0) micrograms/milliliter of chondroitin were significant concentrations that allowing for neurite outgrowth and arborization. The potency of chondroitin in the presence of 10 micrograms/milliliter of aggrecan was then assessed (**Figure 6F**). Concentrations of 0.15625-20.0 micrograms/milliliter of chondroitin was applied with 10 micrograms/milliliter of aggrecan. Data was normalized to the control and was tested for significance with a one-way ANOVA with a Dunnett's *post hoc* test. Similar to when chondroitin was tested without aggrecan, chondroitin concentrations of 5.0, 10.0, and 20.0 micrograms/milliliters significantly increased neurite growth by outcompeting 10.0 micrograms/milliliters of aggrecan, with 20 micrograms/milliliter of chondroitin having a p value <0.001.

After determining from the sholl analysis that LVP2 significantly impacted total neurite outgrowth, LVP2 became our key glycans of interest and was further studied later with concentration-response curves. Similar to the chondroitin, LVP2 alone was applied at various concentrations to neurons, and viability was assessed using a one-way ANOVA with a Dunnett's *post hoc* test (**Figure 6H**).

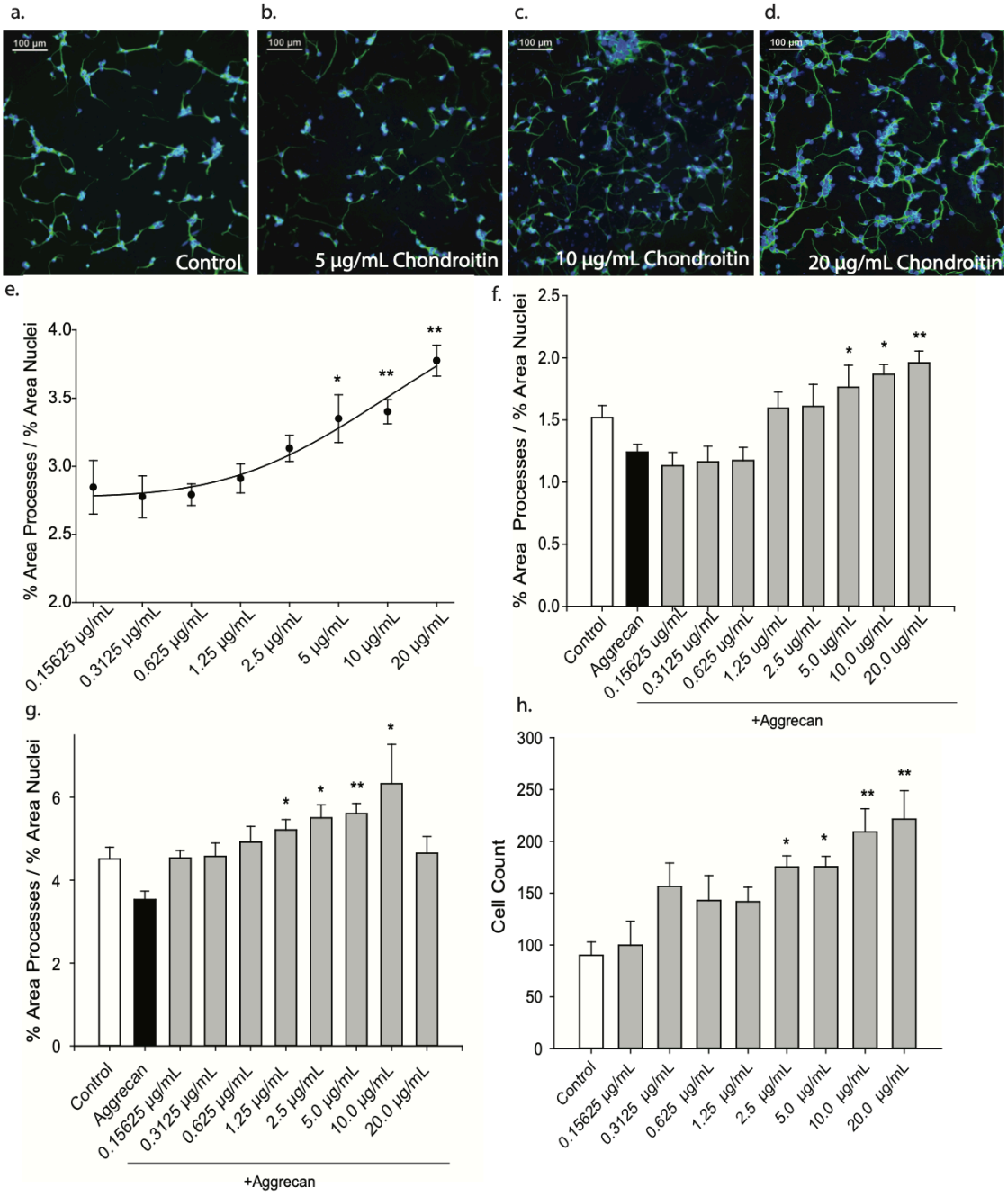

Figure 6: Concentration dependent response of chondroitin and LVP2 on cortical neurite outgrowth. Representative images of cortical neurons treated with water for control (a), 5 µg/mL chondroitin (b), 10 µg/mL chondroitin (c), and 20 µg/mL chondroitin (d). Scale bars represent 100 µm. (e) area analysis of chondroitin concentration curve, *, $p < 0.05$, n=8 (f) area analysis of chondroitin + 10 µg/mL aggrecan concentration curve, *, $p < 0.05$, **, $p < 0.001$, n=8 (g) area analysis of LVP2 + 10 µg/mL aggrecan concentration curve, *, $p < 0.05$, **, $p < 0.001$, n=8 (h) nuclei count of LVP2 + 10 µg/mL aggrecan concentration curve, *, $p < 0.05$, **, $p < 0.001$, n=8

It was determined that 2.5 and 5.0 milligrams/milliliter of LVP2 significantly increased the number of nuclei, with a p value of <0.05, while 10.0 and 20.0 milligrams/milliliter of LVP2 significantly increased the number of nuclei as well with a p value of <0.001. The same concentrations of LVP2 were again applied to cortical neurons, but with the presence of 10.0 micrograms/milliliter of aggrecan (**Figure 6G**). Again, data was assessed with area analysis and statistical analysis was conducted with a one-way ANOVA with Dunnett's *post hoc* test. Concentrations of 1.25, 2.5, 5.0, and 10.0 micrograms/milliliter of LVP2 significantly outcompeted aggrecan to allow for neurite outgrowth. However, 20.0 micrograms/milliliter exhibited a decrease in total processes.

Because of the protective ability the novel glycans exhibited for neurite growth in the presence of aggrecan, the impact of glycans and aggrecan on size and shape of growth cones was tested (**Figure 7**). It was hypothesized that increases growth cone size might have implications for permissive growth environment.

Cortical neurons were treated with increasing concentrations of aggrecan, stained and imaged to view growth cones (**Figure 7D**). Growth cone size was assessed using ROI analysis. Following this, it was determined that increasing concentrations of aggrecan exhibited decreased size in growth cones, and 10.0 micrograms/milliliter of aggrecan exhibited significant decrease of growth cone size. Following this, it became clear that decreased neurite outgrowth is correlated with decreased growth cone size.

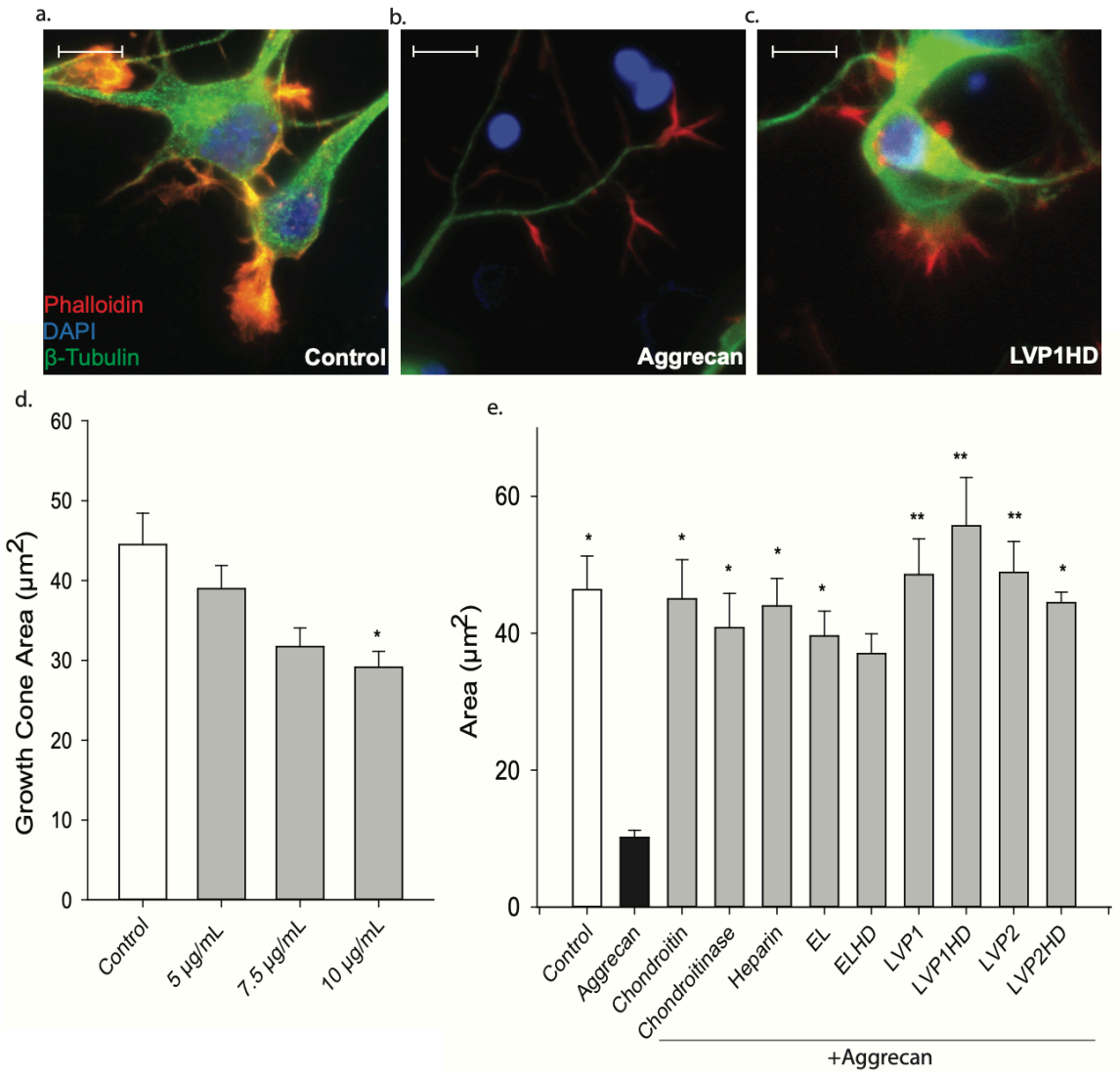

Figure 7: Analysis of growth cones on cortical neurons treated with aggrecan and novel glycans. Representative images of growth cones on cortical neurons treated with water (a), 10 μg/mL aggrecan (b) and 10 μg/mL aggrecan + 10 μg/mL LVP1HD. Scale bars represent 10 μm, neurons were fixed and stained with β-tubulin (green), DAPI (blue), and phalloidin (red). (d) growth cone area analysis done by ROI analysis of cortical neurons treated with water, 5 μg/mL, 7.5 μg/mL, and 10 μg/mL of aggrecan. *, $p < 0.05$, n=24 (e) growth cone area analysis done by ROI analysis of cortical neurons treated with 10 μg/mL aggrecan + 10 μg/mL glycans, *, $p < 0.05$, n=8

Assessment of growth cone size of glycans in the presence of 10.0 micrograms/milliliter of aggrecan was then conducted to determine if glycans outcompeted aggrecan to an extent that exhibited significant increase in growth cone size (**Figure 7E**). Analysis was conducted using a one-way ANOVA was a Dunnett's *post hoc* test, and all glycans tested, except for ELHD, showed significant increases in growth cone size compared to neurons treated solely with aggrecan.

Additional analysis of neurons treated with aggrecan for one week, instead of 48 hours, was conducted to assess if aggrecan continued to exhibit its inhibitory effects of total neurite outgrowth in a long-term effect (**Figure 8A**). After conducting a one-way ANOVA, it was found that 5.0, 7.5, and 10.0 micrograms/milliliter of aggrecan exhibited a significant decrease in neurite outgrowth even one week after plating, thus supporting that the effects of aggrecan on neurite outgrowth are both immediate and long-term.

The mRNA expression of pathways that allow for neurite outgrowth was assessed using qPCR. Specifically, expression of PTPRS, PTPRF, RTN4R, RTN4RL1, and RTN4RL2 was examined in 7-day old neurons to possible determine what mechanism lies behind the glycans that provide the best potential for neurite growth, plasticity, and differentiation. Gene expression fold change was normalized to GAPDH for comparison of gene expression levels, and neurons were assessed in comparison to either water for control, chondroitin, and LVP2HD (**Figure 9**).

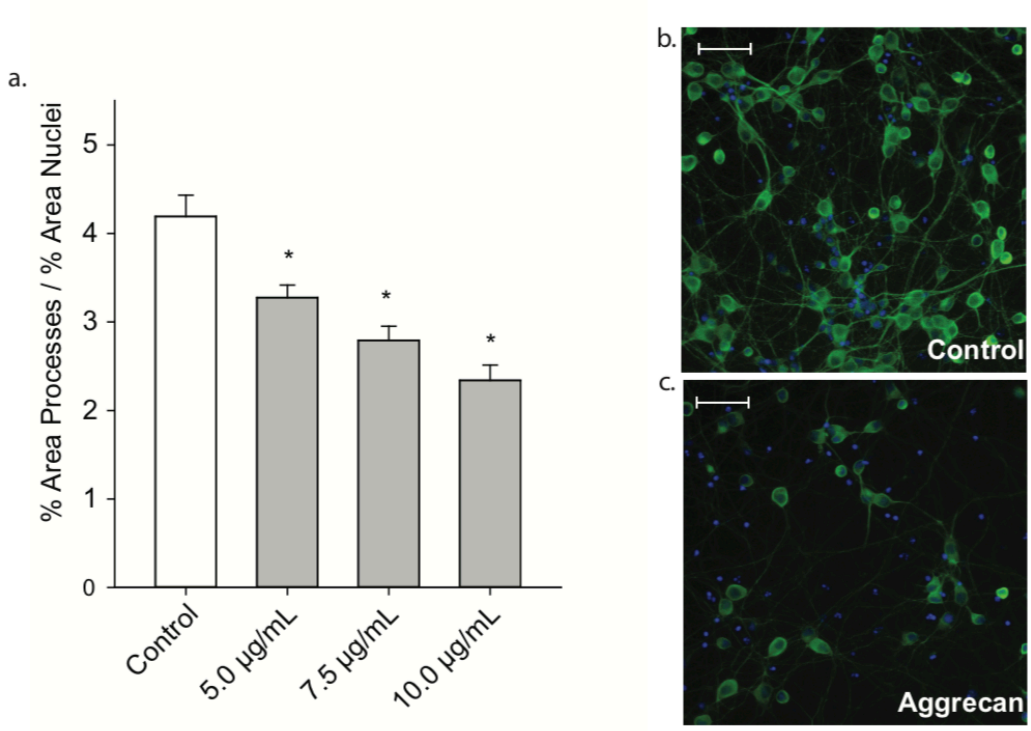

Figure 8: 7-day growth analysis (a) area analysis of cortical neurons treated with water, 5 µg/mL, 7.5 µg/mL, and 10 µg/mL of aggrecan for one week. *, $p < 0.05$, n=8 Representative images of cortical neurons treated with water (b) and 10 µg/mL of aggrecan (c) for one week. Scale bar represents 50 µm.

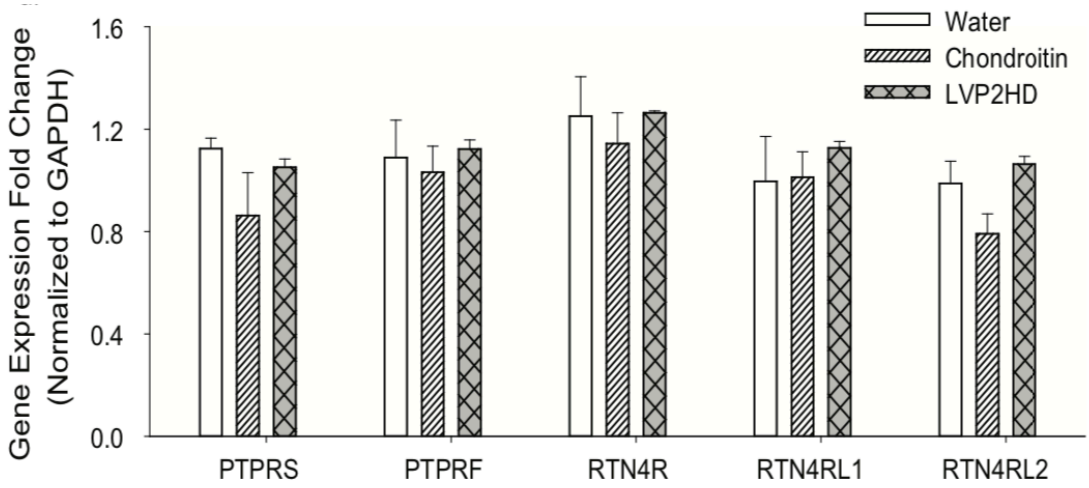

Figure 9: Gene expression fold change normalized to GAPDH on water, chondroitin, and LVP2HD in the absence of aggrecan; n=5

Chondroitin was utilized for comparison in gene expressed due to copious amounts of previous literature confirming our findings of its growth permitting properties. LVP2HD had proven to provide the greatest growth permission of all glycans testing, making it the reason why it was also a candidate for gene analysis.

PTPRS and PTPRF are genes that regulate a variety of cellular processes such as cell growth, differentiation, cell-to-cell interaction, axon generation, and axon guidance (Shen, 2009). Nogo 66 receptors such as RTN4R, RTN4RL1, and RTN4RL2 are responsible for encoding the receptor that medicates axonal regeneration and plasticity in the CNS (Fournier, 2001). Data was normalized to control and following analysis it was determined that there was no difference in PTPRS, PTPRF, RTN4R, RTN4RL1, and RTN4RL2 between control, chondroitin, and LVP2HD.

In addition to the novel glycans from the marine organisms, a preliminary study to examine the effect of chondroitin sulfates with varying lengths on neurite outgrowth was conducted. The goal was to determine if oligosaccharides [n] residues in length would have an impact on neurite outgrowth, or if there was a correlation in length and neurite outgrowth. These glycans were provided by Dr. Joshua Sharp's laboratory.

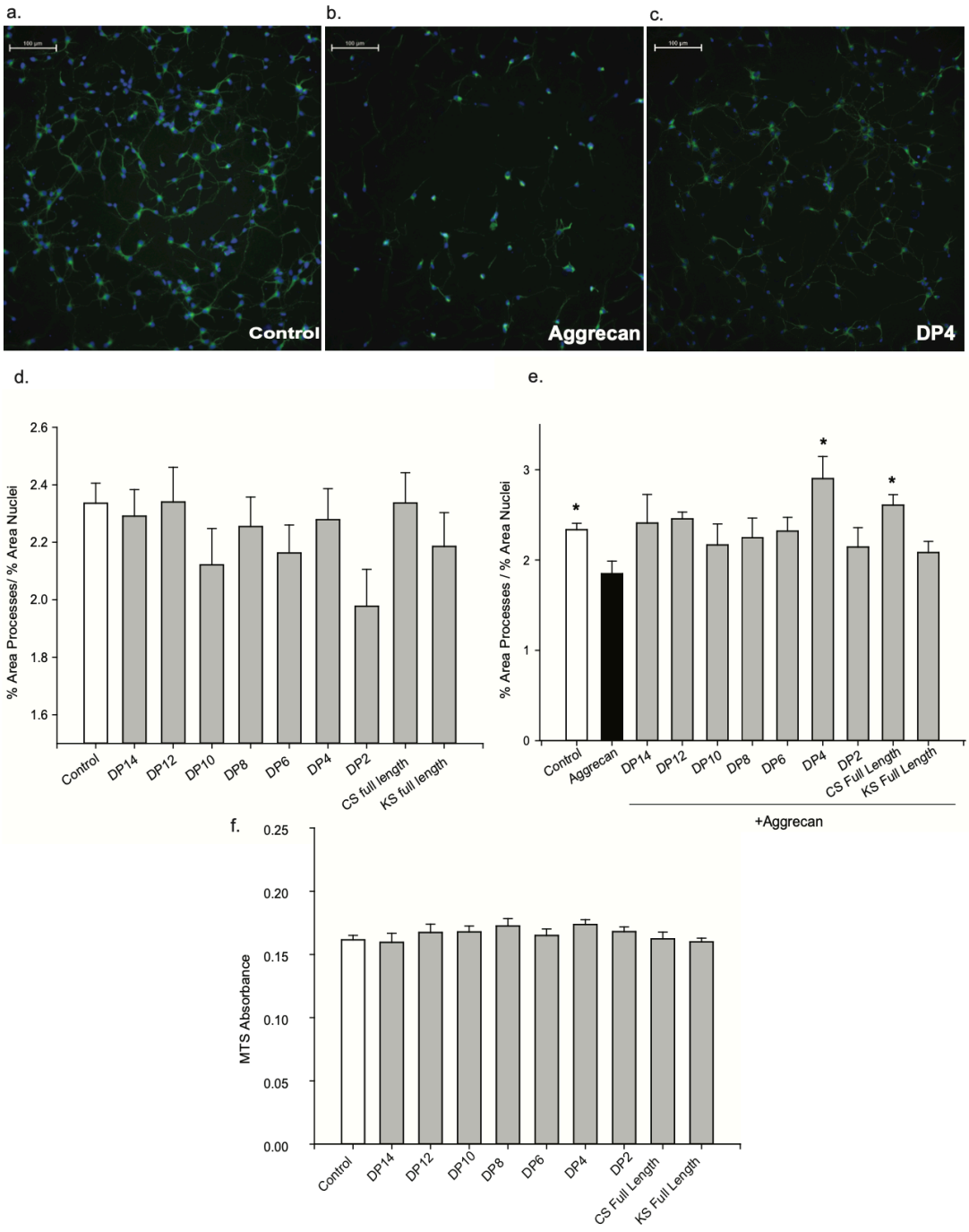

Figure 10: Chondroitin sulfates at varying [n]'s weight analysis. Representative images of cortical neurons treated with water for control (a), 10 μg/mL aggrecan (b), and 10 μg/mL DP4 (992 g/mol) chondroitin (c). Scale bars represent 100 μm. (d) area analysis of chondroitin sulfates with varying lengths impact on cortical neurite outgrowth alone, n=8-16 (e) area analysis of chondroitin sulfates with varying lengths impact on cortical neurite outgrowth in presence of 10 μg/mL aggrecan, *, $p < 0.05$, n=8-16 (f) MTS absorbance assay for toxicity assay on 10 μg/mL chondroitin sulfates with varying lengths, n=8-16

Partially depolymerized chondroitin sulfates from 503 g/mol to 3472 g/mol, as well as full length CS and KS were applied to cortical neurons without the presence of aggrecan, and total neurite outgrowth was assessed using area analysis with one-way ANOVA and Dunnett's *post hoc* versus control (**Figure 10D**). One-way ANOVA failed amongst all groups and showed no significant impact on neurite outgrowth. Area analysis was conducted on cut chondroitin sulfates in the presence of aggrecan, with a one-way ANOVA with Dunnett's *post hoc* test versus aggrecan for control (**Figure 10E**). Following analysis, full length CS and 992g/mol partially depolymerized chondroitin sulfate exhibited significant increases in total neurite outgrowth in the presence of aggrecan.

An MTS absorbance assay was also conducted on the partially depolymerized chondroitin sulfate to confirm that none of the samples showed toxicity to neuronal outgrowth (**Figure 10F**). A one-way ANOVA with a Dunnett's *post hoc* test versus control exhibited no differences on groups, thus demonstrating that no samples were toxic.

IV. Discussion

The data show that several novel sulfated glycans provided rescuing effects on neurite outgrowth *in vitro* against aggrecan. Additionally, the novel glycans exhibited increasing neurite outgrowth in a concentration dependent manner. The overall increase in axonal growth in the presence of both aggrecan and novel glycans suggest that the glycans allow the environment to be growth permissive, indicating that the glycans may provide a potential window for plasticity following the upregulation of KS/CSPGs with injury. Data from chondroitin sulfates with varying [n] residues indicate that size of glycan and neurite outgrowth are not related.

In accordance with the growth cone data, increasing concentrations of aggrecan lead to smaller growth cones, while nearly all neuron cultures treated with aggrecan and novel glycans exhibited a significant increase in growth cone size and shape. Previous studies have confirmed that CS/KSPGs stop or stall the development of growth cones and act as a barrier to growth cone advances (Snow et al., 1990, Wu et al., 1992). This growth inhibitory mechanism may be indicative of neuronal regeneration (Hynds, 1999). It has also been previously discussed that the regulation of growth cones through CSPGs may be dependent on the structure and conformation of the CSPG, and that CSPGs may affect growth cones by possibly binding directly to the growth cone (Snow, 1996) Surprisingly, qPCR data revealed no change in expression of PTPRS, PTPRF, RTN4R, RTN4RL1, and RTN4RL2. PTPRS and PTPRF are leukocyte common antigen-related (LAR) subfamily of receptors that modulate neuronal development and axonal regeneration (Uetani, 2006). PTPRS is a major CSPG receptor in sympathetic neurons, and previous research has

revealed that the absence of PTPRS restores axon outgrowth (Gardner, 2013). The results depicting no change in PTPRS expression when treated with novel glycans indicate that the novel glycans do not affect neurite outgrowth by alterative of PTPRS receptors. Furthermore, the results demonstrating the absence of change in expression of PTPRF indicate that the novel glycans do not alter neurite outgrowth by interaction of the LAR receptors. Previous research has indicated that CSPGs bind to Nogo receptors (RTN4R, RTN4RL1, RTN4RL2) for myelin associated growth inhibition (Sharma, 2012). Overall, the expression of these genes was not altered at day 7 *in vitro;* however, it is possible that these genes were alters in the first day or two of culture and set the cascade. In order to further explore this, the expression of these genes and proteins should be quantified throughout the growth periods of culture. Additionally, changes in the function of the receptors may need to be tested in order to provide insight on the mechanism of action for these novel glycans to allow for neurite outgrowth.

Previous research regarding CSPGs as neurite outgrowth modulators indicate that Nogo receptors are novel receptors for CSPGs, which may provide an insight into the mechanism of CSPG inhibition (Dickendesher, 2012). Therefore, it is understandable that CSPG inhibition may not be due to decreases in Nogo receptor expression, but due to the binding of CSPGs to the receptors itself. PTPRS, another previously identified CSPG receptor, plays a role in converting growth cones into a dystrophic state by tightly binding them with CSPG substrates, thus bringing a deeper understanding of the role of PTPRS in the mediation of growth of neurons (Lang, 2015). With the possibility of PTPRS being a possible therapeutic in relieving CSPG-mediated inhibition, our data demonstrates that the expression of the genes are not impacted by CSPGs, but rather

perhaps the mechanism by which CSPGs interact with PTPRS and other genes may be affected.

Limitations of Experiment

Because this study was only conducted *in vitro*, it is unknown if these novel glycans can continue to exhibit its neuroprotective properties in the living system. It is important to conduct *in vivo* testing in order to determine possible side effects and the total effects the treatment may have on human health. With this in mind, an *in vivo* test with induced glial scarring following injury may provide monumental data and information regarding glycans influence on breaking down the CS/KSPG barrier formed following TBI or SCI. Additionally, this study could have also been done *in vitro* with astrocytes present to help recapitulate more of the cellular dynamics one would expect to see if the astrocytes would respond to the glycans and thereby alter neurons indirectly.

Many of the treatments changed in cell number, so changes in neurite size could be confounded by the cell-number. The number of cells that was plated on the first day remained the same in each well. The differences in cell number are likely attributed to survival upon plating. However, when performing calculations and data analysis, data was normalized to total nuclei coverage to allow distinct separation between cell number and neurite outgrowth. This method of analysis reduces confounding variables, however we cannot rule out that differences in growth may be influenced by changes in cell density, as neurons frequently display contact inhibition.

Future Directions

Further directions include investigation of novel glycan structure, to perhaps understand the mechanism behind the interaction of novel sulfated glycans and neurite outgrowth. Since sulfation patterns directly influence conformation and dynamics, continuing to elucidate sulfation pattern structure-function in novel glycans may be important in understanding ECM interactions. Addressing the variation in novel glycan sulfation patterns, size, dynamics, and conformation by utilizing liquid-state nuclear magnetic resonance (NMR), spectroscopy, scalar coupling constant, nuclear overhauser effect (NOE) profiles, and other models of analysis to explore the dynamics of molecular interactions in neurite regeneration. Investigation of a combination of differentiating sulfation patterns and neurite growth promoting abilities of novel glycans can allow for further investigation of the structure of those that rescued structure the most in response to neurite growth inhibition due to CS/KSPGs.

In vivo testing will provide further insight into possible biomedical functions of the novel sulfated glycans, and may help determine what glycan provides the best potential for neurite growth, plasticity, and differentiation. Further analysis of growth cone shape and size may provide further insight on the mechanism of the interaction of novel glycans with neurite outgrowth. Filopodia projections have been linked to dendrite creation when new synapses are formed in the brain, while lamellipodia seem designed for persistent protrusion over a surface.

Analysis of changes of dendritic spines may provide further insight into the plasticity of neurite outgrowth and the mechanism by which novel glycans may allow for

neurite outgrowth. Dendritic spines are considered as excitatory postsynaptic sites that express high levels of plasticity, and morphology of spines correlate with the level of plasticity (De Vivo, 2013).

The size and shape of spines correlate with calcium kinetics in the spines, which may be significant for regulating the communication between synapses (Hering, 2002). Specifically, filopodial protrusions indicate novel excitatory synapses, and filopodial protrusions become increasingly sparse as maturation furthers (De Vivo, 2013). Meanwhile, the shorter spine necks of mushroom and stubby spines may also be of importance. Therefore, classification of spines based on size by cup shape, mushroom, stubby, thin, and filopodium, as well as calcium signaling, may provide further insight into the mechanism behind the novel glycans' impact on neurite outgrowth.

Previous studies have demonstrated that CSPGs restrain motility of dendritic spines, and that degradation of CSPGs allow for the potentiation of existing synapses (De Vivo, 2013). With this in mind, we hypothesize that analysis of dendritic spines of neurite treated with CSPGs such as aggrecan and novel glycans will ultimately lead to potentiation of synapses and increased motility of dendritic spines.

Overall Conclusions

Sulfated glycans, both from marine life and other sources, possess significant potential to outcompete the growth inhibitory CS/KSPG barrier. The exact molecular mechanism by which these glycans exert their neurostimulatory effects is unknown, but further studies of glycan structure and sulfation may provide more insight into the

mechanism. Results may tentatively provide an insight on the mechanism of neurite inhibition and regeneration, as well as cell-to-cell communication in the central nervous system. This may open the opportunity for a greater understanding of proteoglycans as critical regulators of cell structure in plants and animals, and may allow for further studies aimed at developing pharmacological agents that may treat spinal cord or brain injuries.

LIST OF REFERENCES

Ashpole, Nicole M., and Andy Hudmon. “Excitotoxic Neuroprotection and Vulnerability with CaMKII Inhibition.” *Molecular and Cellular Neuroscience*, vol. 46, no. 4, Feb. 2011, pp. 720–730., doi:10.1016/j.mcn.2011.02.003.

Barritt, A W et al. “Chondroitinase ABC promotes sprouting of intact and injured spinal systems after spinal cord injury.” *The Journal of Neuroscience : the official journal of the Society for Neuroscience* vol. 26,42 (2006): 10856-67. doi:10.1523/JNEUROSCI.2980-06.2006

Beller, J. A., & Snow, D. M. (2014). Proteoglycans: Road signs for neurite outgrowth. *Neural Regeneration Research*, *9*(4), 343–355. https://doi.org/10.4103/1673-5374.128235

Clement, A., Sugahara, K., & Faissner, A. (1999). Chondroitin sulfate E promotes neurite outgrowth of rat embryonic day 18 hippocampal neurons. *Neuroscience Letters*, *269*(3), 125–128.

Collin, E. C., Carroll, O., Kilcoyne, M., Peroglio, M., See, E., Hendig, D., … Pandit, A. (2017). Ageing affects chondroitin sulfates and their synthetic enzymes in the intervertebral disc. *Signal Transduction and Targeted Therapy*, *2*(July), 4–11. https://doi.org/10.1038/sigtrans.2017.49

Daniell, H. (2012). *CNS Injury, Glial Scars, and Inflammation: Inhibitory extracellular matrices and regeneration failureccess*. *76*(October 2009), 211–220. https://doi.org/10.1007/s11103-011-9767-z.Plastid

de Vivo, L., Landi, S., Panniello, M. *et al.* Extracellular matrix inhibits structural and functional plasticity of dendritic spines in the adult visual cortex. *Nat Commun* **4,** 1484 (2013). https://doi.org/10.1038/ncomms2491

Dickendesher, Travis L et al. "NgR1 and NgR3 are receptors for chondroitin sulfate proteoglycans." *Nature neuroscience* vol. 15,5 703-12. 11 Mar. 2012, doi:10.1038/nn.3070

Djerbal, L., Lortat-Jacob, H., & Kwok, J. (2017). Chondroitin sulfates and their binding molecules in the central nervous system. *Glycoconjugate Journal*, *34*(3), 363–376. https://doi.org/10.1007/s10719-017-9761-z

Fournier AE, GrandPre T, Strittmatter SM. Identification of a receptor mediating Nogo-66 inhibition of axonal regeneration. Nature. 2001;409(6818):341–346.

Gardner, R. T., & Habecker, B. A. (2013). Infarct-Derived Chondroitin Sulfate Proteoglycans Prevent Sympathetic Reinnervation after Cardiac Ischemia-Reperfusion Injury. *The Journal of Neuroscience*, *33*(17), 7175 LP – 7183. https://doi.org/10.1523/JNEUROSCI.5866-12.2013

Harris, N G et al. "Traumatic brain injury results in disparate regions of chondroitin sulfate proteoglycan expression that are temporally limited." *Journal of Neuroscience Research* vol. 87,13 (2009): 2937-50. doi:10.1002/jnr.22115

Hering, Heike & Sheng, Morgan. (2002). Dendritic Spines: Structure, Dynamics and Regulation. Nature reviews. Neuroscience. 2. 880-8. 10.1038/35104061.

Holmes, M W et al. “Hyaluronic acid in human articular cartilage. Age-related changes in content and size.” *The Biochemical journal* vol. 250,2 (1988): 435-41. doi:10.1042/bj2500435

Hynds DL, Snow DM. Neurite outgrowth inhibition by chondroitin sulfate proteoglycan: Stalling/stopping exceeds turning in human neuroblastoma growth cones. Exp Neurol. 1999;160:244–255.

Jin, J., Tilve, S., Huang, Z., Zhou, L., Geller, H. M., & Yu, P. (2018). Effect of chondroitin sulfate proteoglycans on neuronal cell adhesion, spreading and neurite growth in culture. *Neural Regeneration Research*, *13*(2), 289–297. https://doi.org/10.4103/1673-5374.226398

Johnson, W. E. B., Caterson, B., Eisenstein, S. M., Hynds, D. L., Snow, D. M., & Roberts, S. (2002). Human intervertebral disc aggrecan inhibits nerve growth in vitro. *Arthritis & Rheumatology*, *46*(10).

Keough, M. B., Rogers, J. A., Zhang, P., Jensen, S. K., Stephenson, E. L., Chen, T., … Yong, V. W. (2016). An inhibitor of chondroitin sulfate proteoglycan synthesis promotes central nervous system remyelination. *Nature Communications*, *7*, 1–12. https://doi.org/10.1038/ncomms11312

Kim, Byung G et al. “Degradation of chondroitin sulfate proteoglycans potentiates transplant-mediated axonal remodeling and functional recovery after spinal cord injury in adult rats.” *The Journal of comparative neurology* vol. 497,2 (2006): 182-98. doi:10.1002/cne.20980

Lang, Bradley T et al. “Modulation of the proteoglycan receptor PTPσ promotes recovery after spinal cord injury.” *Nature* vol. 518,7539 (2015): 404-8. doi:10.1038/nature13974

Lindahl U, Couchman J, Kimata K, et al. Proteoglycans and Sulfated Glycosaminoglycans. 2017. In: Varki A, Cummings RD, Esko JD, et al., editors. Essentials of Glycobiology [Internet]. 3rd edition. Cold Spring Harbor (NY): Cold Spring Harbor Laboratory Press; 2015-2017. Chapter 17. Available from: https://www.ncbi.nlm.nih.gov/books/NBK453033/doi: 10.1101/glycobiology.3e.017

Millipore Sigma, [Structural Proteins – Aggrecan]. Retrieved from https://www.sigmaaldrich.com/life-science/metabolomics/enzyme-explorer/learning-center/structural-proteins/aggrecan.html.

Miura, Y., & Endo, T. (2016). Glycomics and glycoproteomics focused on aging and age-related diseases - Glycans as a potential biomarker for physiological alterations. *Biochimica et Biophysica Acta - General Subjects*, *1860*(8), 1608–1614. https://doi.org/10.1016/j.bbagen.2016.01.013

Ohtake, Yosuke, and Shuxin Li. “Molecular mechanisms of scar-sourced axon growth inhibitors.” *Brain research* vol. 1619 (2015): 22-35. doi:10.1016/j.brainres.2014.08.064

Pomin, V. H., Park, Y., Huang, R., Heiss, C., Sharp, J. S., Azadi, P., & Prestegard, J. H. (2012). Exploiting enzyme specificities in digestions of chondroitin sulfates A

and C: Production of well-defined hexasaccharides. *Glycobiology*, *22*(6), 826–838. https://doi.org/10.1093/glycob/cws055

Pomin, V. (2014). Marine medicinal glycomics. *Frontiers in Cellular and Infection Microbiology*, *4*, 5. https://doi.org/10.3389/fcimb.2014.00005

Queiroz, I. N., Wang, X., Glushka, J. N., Santos, G. R., Valente, A. P., Prestegard, J. H., … Pomin, V. H. (2015). Impact of sulfation pattern on the conformation and dynamics of sulfated fucan oligosaccharides as revealed by NMR and MD. *Glycobiology*, *25*(5), 535–547. https://doi.org/10.1093/glycob/cwu184

Riss TL, Moravec RA, Niles AL, et al. Cell Viability Assays. 2013 May 1 [Updated 2016 Jul 1]. In: Sittampalam GS, Coussens NP, Brimacombe K, et al., editors. Assay Guidance Manual [Internet]. Bethesda (MD): Eli Lilly & Company and the National Center for Advancing Translational Sciences; 2004-. Available from: https://www.ncbi.nlm.nih.gov/books/NBK144065/

Sato, Y., & Endo, T. (2010). Alteration of brain glycoproteins during aging. *Geriatrics and Gerontology International*, *10*(SUPPL. 1). https://doi.org/10.1111/j.1447-0594.2010.00602.x

Sharma, Kartavya et al. “Scar-mediated inhibition and CSPG receptors in the CNS.” *Experimental neurology* vol. 237,2 (2012): 370-8. doi:10.1016/j.expneurol.2012.07.009

Shen Y, et al. PTPsigma is a receptor for chondroitin sulfate proteoglycan, an inhibitor of neural regeneration. Science. 2009;326:592–596. doi: 10.1126/science.1178310.

Shida, M., Mikami, T., ichi Tamura, J., & Kitagawa, H. (2017). A characteristic chondroitin sulfate trisaccharide unit with a sulfated fucose branch exhibits neurite outgrowth-promoting activity: Novel biological roles of fucosylated chondroitin sulfates isolated from the sea cucumber Apostichopus japonicus. *Biochemical and Biophysical Research Communications*, *487*(3), 678–683. https://doi.org/10.1016/j.bbrc.2017.04.114

Snow, DM, Steindler, DA., Silver, J., (1990). Molecular and cellular charactierization of the glial roof plate of the spinal cord and optic tectum: a possible role for a proteoglycan in the development of an axon barrier. Dev. Biol. 138: 359-376.

Snow, D.M. and Letourneau, P.C. (1992), Neurite outgrowth on a step gradient of chondroitin sulfate proteoglycan (CS-PG). J. Neurobiol., 23: 322-336. doi:10.1002/neu.480230311

Snow, Diane & Brown, Eric & Letourneau, Paul. (1996). Growth cone behavior in the presence of soluble chondroitin sulfate proteoglycan (CSPG), compared to behavior on CSPG bound to laminin or fibronectin. International journal of developmental neuroscience : the official journal of the International Society for Developmental Neuroscience. 14. 331-49. 10.1016/0736-5748(96)00017-2.

Varki A, Cummings RD, Esko JD, et al., editors. Essentials of Glycobiology [Internet]. 3rd edition. Cold Spring Harbor (NY): Cold Spring Harbor Laboratory Press; 2015-2017. doi: 10.1101/glycobiology.3e.017

Uetani, N., Chagnon, M. J., Kennedy, T. E., Iwakura, Y., & Tremblay, M. L. (2006). Mammalian Motoneuron Axon Targeting Requires Receptor Protein Tyrosine Phosphatases σ and δ. *The Journal of Neuroscience*, *26*(22), 5872 LP – 5880. https://doi.org/10.1523/JNEUROSCI.0386-06.2006

Vasconcelos, A. A., Sucupira, I. D., Guedes, A. L., Queiroz, I. N., Frattani, F. S., Fonseca, R. J., & Pomin, V. H. (2018). Anticoagulant and antithrombotic properties of three structurally correlated sea urchin sulfated glycans and their low-molecular-weight derivatives. *Marine Drugs*, *16*(9), 1–14. https://doi.org/10.3390/md16090304

Wu, D-Y., Silver, J., Schneider, JE., Jharveri, S. (1991). The barrier function of tectal midline glial cells and its association with proteoglycan distribution. Soc Neurosci Abstr 17: 741.